TRIBOLOGICAL, MECHANICAL AND ELECTROCHEMICAL CHARACTERIZATION OF GS-42CrMo4V TRACK ROLLER STEEL FOR MINING APPLICATIONS

K. KRISHNAKUMAR[1,2], M. R. RAJAMANICKAM[2]

[1]Centre for Applied Research & Development (CARD), NLC India Limited, Neyveli, 607807, India

[2] Department of Mechanical Engineering, Annamalai University, Annamalai Nagar, 608 002, India

Abstract: Track rollers used in bucket wheel excavators are subjected to repeated mechanical loading in an environment where abrasive particles, moisture and corrosive contaminants can accelerate surface deterioration. The present study examines the mechanical, electrochemical and tribological behaviour of GS-42CrMo4V cast steel used for this application. The material was characterized through chemical composition analysis, microhardness measurement, tensile testing and fractographic examination. Its corrosion behaviour was further evaluated in 3.5 wt.% NaCl and acidic HCl and H_2SO_4 solutions using potentiodynamic polarization and electrochemical impedance spectroscopy, while three-body abrasion and reciprocating wear tests were carried out to assess its resistance to material loss under different contact conditions. The bottom roller exhibited an average microhardness of 430 HV, compared with 314.2 HV for the roller pin. Tensile and fractographic observations indicated good mechanical performance, although localized damage features were observed on the fractured surfaces. The electrochemical results showed that the material performed better in the neutral chloride solution than in the acidic media. In 3.5 wt.% NaCl, the corrosion current density and corrosion rate were 1.597 µA cm^{-2} and 0.487 mpy, respectively, whereas the acidic solutions produced considerably higher corrosion activity. The wear tests confirmed that high hardness alone did not prevent material removal under abrasive and sliding contact. Abrasive action, plastic deformation and localized adhesive interactions contributed to surface degradation under the investigated conditions. The results therefore indicate that, despite its favourable hardness and mechanical characteristics, GS-42CrMo4V remains susceptible to degradation in aggressive acidic environments and under severe abrasive and sliding conditions. The observed behaviour points to the need for further improvement in material processing, surface condition, corrosion protection and the control of abrasive particle ingress. These findings provide a basis for understanding the service-related limitations of the material and for improving the durability of track rollers used in mining equipment.

[DOI: 10.22068/ijmse.4652]

Keywords: GS-42CrMo4V; track roller; bucket wheel excavator; corrosion behaviour; electrochemical impedance spectroscopy; abrasive wear; mining equipment

1. Introduction

Bucket wheel excavators (BWEs) are among the major continuous mining systems used for large-scale surface excavation and material handling [1]. Their reliable operation depends on several mechanical systems, including the crawler undercarriage. Within this assembly, track rollers support and transmit substantial static and dynamic loads between the machine structure and the track system. During operation, the rollers are subjected to repeated contact loading, impact, abrasive particle intrusion, and environmental exposure. These conditions can cause progressive material degradation and contribute to premature component failure, increased maintenance requirements, and loss of equipment availability [2].

The service environment of a track roller is challenging because mechanical loading is accompanied by continuous surface interaction with the track and possible ingress of soil, rock fragments, dust, and moisture. The material must therefore possess adequate strength and hardness while retaining sufficient resistance to wear and other forms of surface damage. Previous investigations have emphasized that the structure, material selection, and processing of roller components are important factors governing their service life under severe crawler operating conditions [3].

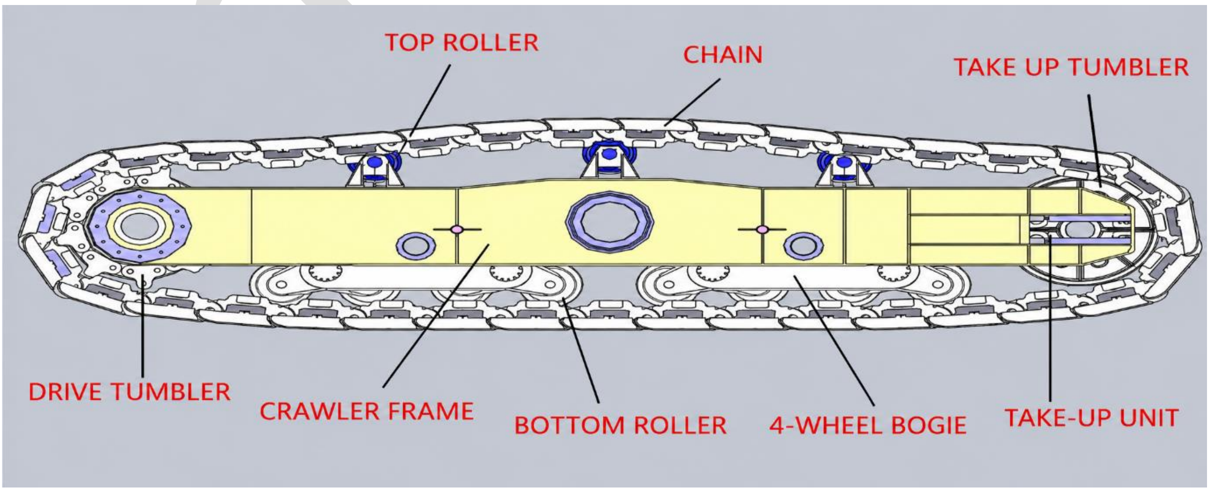

Fig. 1. Schematic representation of a bucket wheel excavator crawler system showing the location of the track rollers.

[DOI: 10.22068/ijmse.4652]

Low-alloy chromium–molybdenum steels are widely used in heavily loaded engineering applications because their mechanical properties can be customized through alloy design and heat treatment. These steels are used in components where strength, hardenability, toughness, and resistance to deformation are required simultaneously [4]. GS-42CrMo4V cast steel belongs to this family of materials and is suitable for applications involving repeated contact loading and abrasive conditions. The response of such steels, however, depends not only on nominal chemical composition but also on the material condition and microstructural characteristics developed during manufacturing and subsequent heat treatment. These factors influence the balance among hardness, strength, ductility, and resistance to degradation during service [5], [6].

Wear is one of the major factors affecting the durability of mining and earthmoving components [7]. Under abrasive conditions, hard particles entering the contact region may remove material through micro-cutting, micro-ploughing, and micro-fracture mechanisms [8], [9]. The resulting wear rate is influenced by several variables, including abrasive characteristics, contact pressure, surface condition, hardness, and microstructural features of the material. Hardness is therefore an important parameter, but it cannot independently predict wear resistance under all service condition [10], [11]. Changes in load, temperature, contact conditions, and the nature of the wear debris may alter the dominant degradation mechanism and, consequently, the rate of material loss [9], [12].

The environmental condition can further influence the long-term performance of track roller materials. Exposure to moisture, dissolved salts, and chemically aggressive contaminants may initiate electrochemical reactions and progressively affect surface integrity. The severity of corrosion is strongly dependent on the electrolyte composition and environmental chemistry. For this reason, the corrosion behaviour of an engineering material should be assessed under relevant conditions rather than inferred solely from its nominal alloy composition [13]. Potentiodynamic polarization provides information on the relative corrosion tendency of a material, whereas electrochemical impedance spectroscopy can be used to examine the resistance of the electrode interface and the electrochemical processes occurring at the material surface [13], [14].

[DOI: 10.22068/ijmse.4652]

In practical applications, wear and corrosion may not act independently. Mechanical contact can remove surface films and expose fresh metallic surfaces, while corrosion can modify the near-surface condition and facilitate subsequent mechanical damage. The combined action of these processes, generally described as tribocorrosion, can result in degradation that is more complex than either corrosion or wear considered separately [15]. This interaction is relevant to mining equipment, where repeated loading, abrasive contamination, and environmental exposure may occur during the same service period.

Although chromium–molybdenum steels have been widely studied, published work often considers mechanical properties, corrosion resistance, and tribological behaviour as separate aspects of material performance. Studies specifically examining GS-42CrMo4V cast steel used in bucket wheel excavator track rollers are comparatively limited. More importantly, the available experimental information is not always translated into a clear assessment of the material limitations relevant to component service or into practical approaches for improving durability.

The present study therefore investigates GS-42CrMo4V cast steel used in a bucket wheel excavator track-roller system through chemical composition analysis, microhardness measurement, tensile testing, fractographic examination, electrochemical evaluation, and tribological testing. The electrochemical behaviour is examined in chloride and acidic environments, while the tribological response is assessed under abrasive and reciprocating contact conditions. The purpose of the work is to use the experimental results for identifying the principal limitations indicated by the mechanical, electrochemical, and wear responses of the material and to examine their implications for track-roller service.

Based on the observed behaviour, possible routes for improving component durability are subsequently discussed. These include material and heat-treatment optimization, improvement of surface condition where justified by the experimental findings, protection against aggressive environmental exposure, and reduction of abrasive particle ingress into the contact region. The distinction between the results obtained experimentally and the improvement strategies proposed from those results is maintained throughout the study.

[DOI: 10.22068/ijmse.4652]

2. Experimental Methods and Results

2.1 Material and Specimen Preparation

The material investigated in the present study was GS-42CrMo4V cast steel used for the bottom roller of a bucket-wheel excavator crawler system. The investigated specimens are collected from the failed bottom roller. A roller-pin material from the same track assembly was also examined for comparison of mechanical characteristics.

The bottom roller taken up for the study is subjected to quenching and tempering followed by case hardening on the working surface. The specified surface hardness is approximately 375–425 BHN with a nominal hardened depth of 4 mm.

Specimens for chemical, mechanical, fractographic, electrochemical and tribological characterization were prepared from the failed bottom rollers. The specimen surfaces used for electrochemical measurements were sequentially ground using silicon carbide abrasive papers up to 2400 grit, followed by cleaning with acetone, rinsing with distilled water and drying under ambient laboratory conditions.

2.2 Chemical Composition

The chemical composition of the investigated steel was determined by optical emission spectroscopy. The measured elemental composition is presented in Table 1.

Table 1. Chemical composition of GS-42CrMo4V steel

Element	wt.%
C	0.4270
Si	0.2140
Mn	0.8460
P	0.0056
S	0.0173
Ni	0.0407

[DOI: 10.22068/ijmse.4652]

Element	wt.%
Cr	1.0700
Mo	0.1830
Cu	0.1670
Al	0.0386
Ti	0.0089
V	0.0106

The steel contained 0.427 wt.% C, 1.070 wt.% Cr and 0.183 wt.% Mo, with moderate Mn and Si contents. The carbon content provides a basis for the development of high strength and hardness following hardening, while chromium and molybdenum contribute to hardenability and tempering resistance. The relatively low phosphorus and sulphur contents are favourable for maintaining mechanical integrity. The measured composition therefore provides a suitable alloying basis for a high-strength, wear-resistant cast-steel component.

2.3 Microhardness Behaviour

Microhardness measurements were carried out using a Matsuzawa MMT-X microhardness tester with a test load of 100 gf and a dwell time of 10 s. Three measurements were obtained from representative regions of the bottom roller and roller-pin materials. The measured values and statistical parameters are presented in Table 2.

Table 2. Microhardness of the bottom roller and roller-pin materials

Specimen	Trial 1 (HV)	Trial 2 (HV)	Trial 3 (HV)	Mean (HV)	SD (HV)
Bottom roller	434.0	418.0	438.0	430.0	10.6
Roller pin	315.6	319.0	308.0	314.2	5.6

[DOI: 10.22068/ijmse.4652]

The bottom roller exhibited a mean microhardness of 430.0 ± 10.6 HV, considerably higher than the 314.2 ± 5.6 HV measured for the roller pin. The higher hardness of the roller is consistent with its requirement to withstand repeated rolling and sliding contact together with abrasive interaction. The measured hardness also indicates the presence of a hardened condition in the investigated roller material.

The difference between the roller and pin hardness reflects their different functional requirements within the track assembly. The higher hardness of the roller provides greater resistance to surface deformation and abrasive penetration, whereas the lower hardness of the pin can provide a comparatively more compliant condition for load transfer and service durability.

2.4 Tensile Behaviour

Tensile testing was performed using a Tinius Olsen H50KL universal testing machine. The test was conducted at room temperature using a standard tensile-testing procedure for metallic materials consistent with ASTM E8/E8M. The tensile-strength values obtained from three specimens of each material are summarized in Table 3.

Table 3. Tensile strength of the investigated materials

Component	Sample 1 (MPa)	Sample 2 (MPa)	Sample 3 (MPa)	Mean UTS (MPa)	SD (MPa)
Bottom roller	780	779	761	773.3	10.7
Roller pin	978	888	966	944.0	48.9

The bottom roller exhibited tensile strengths between 761 and 780 MPa, with a mean ultimate tensile strength of 773.3 ± 10.7 MPa. The corresponding values for the roller pin ranged from 888 to 978 MPa, giving a mean of 944.0 ± 48.9 MPa.

The roller-pin material therefore exhibited a higher tensile strength than the bottom roller. This difference is consistent with the different mechanical conditions required for the two components and may be associated with differences in heat treatment and component geometry. The stress-strain

[DOI: 10.22068/ijmse.4652]

responses also indicate deformation prior to final fracture, demonstrating that the investigated materials did not fail through an entirely brittle tensile response. The engineering stress-strain responses obtained from the bottom roller and roller-pin specimens are presented in Fig. 2 and Fig. 3, respectively.

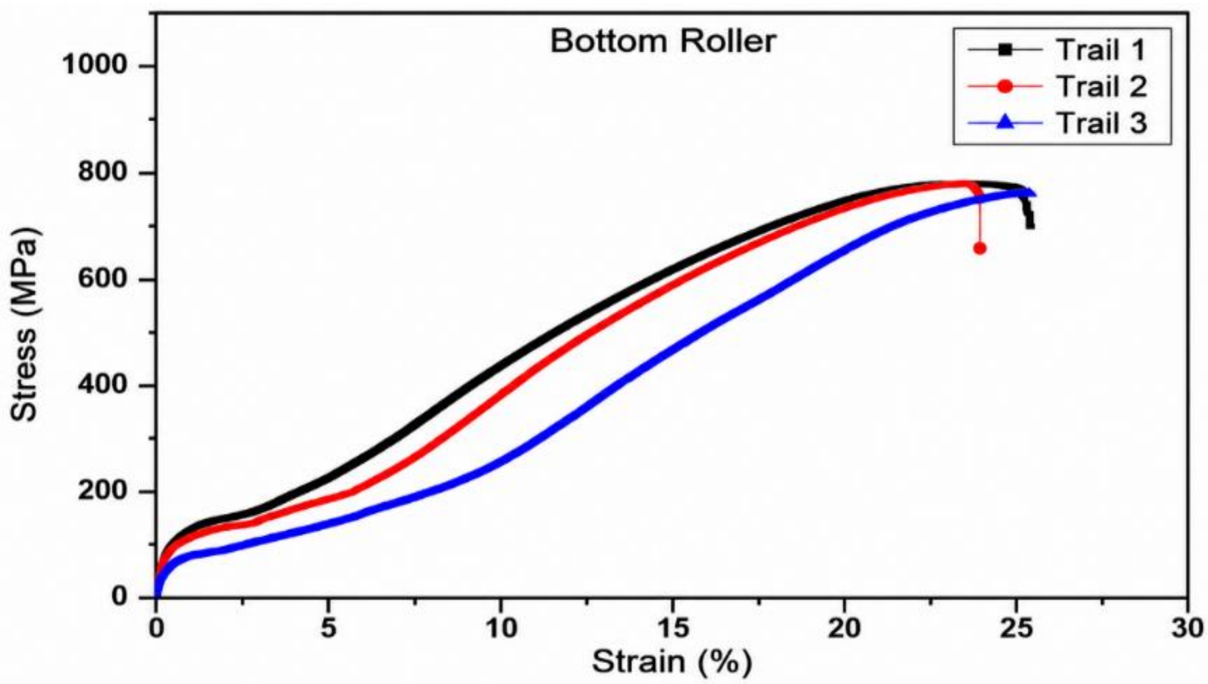

Fig. 2. Engineering stress-strain curves of GS-42CrMo4V bottom roller specimens.

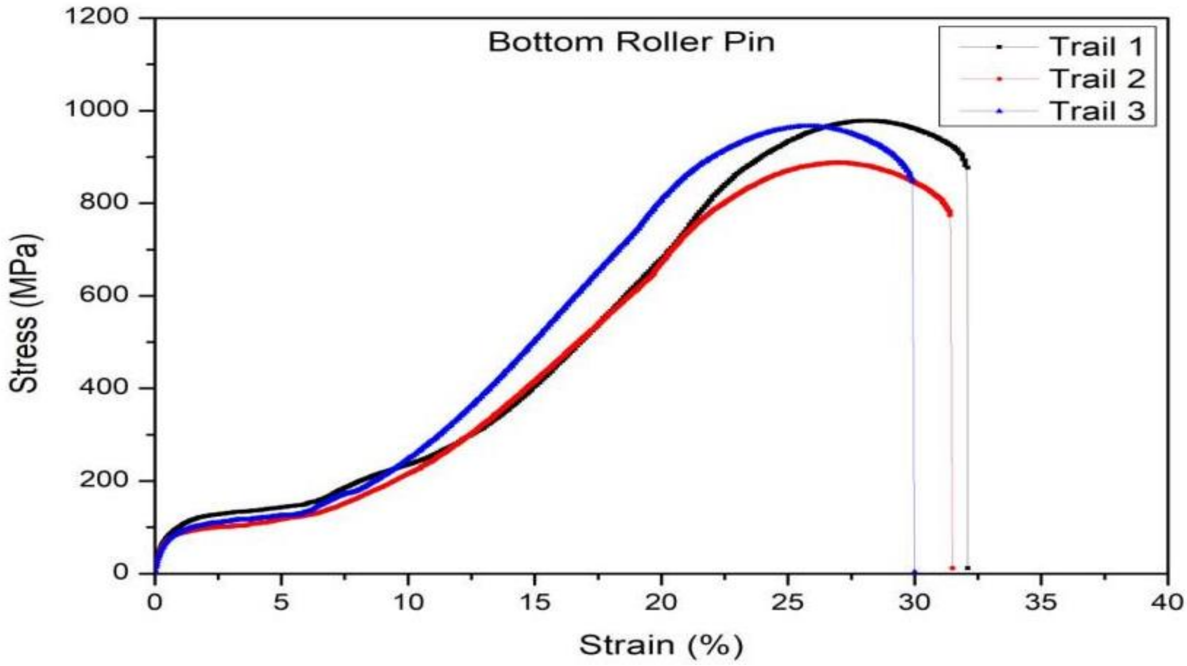

Fig. 3. Engineering stress-strain curves of GS-42CrMo4V roller-pin specimens.

[DOI: 10.22068/ijmse.4652]

2.5 Fractographic Characteristics

Fractographic examination was carried out using scanning electron microscopy to characterize the morphology of the tensile fracture surface. The macroscopic fracture surface and representative SEM morphology are shown in Fig. 4.

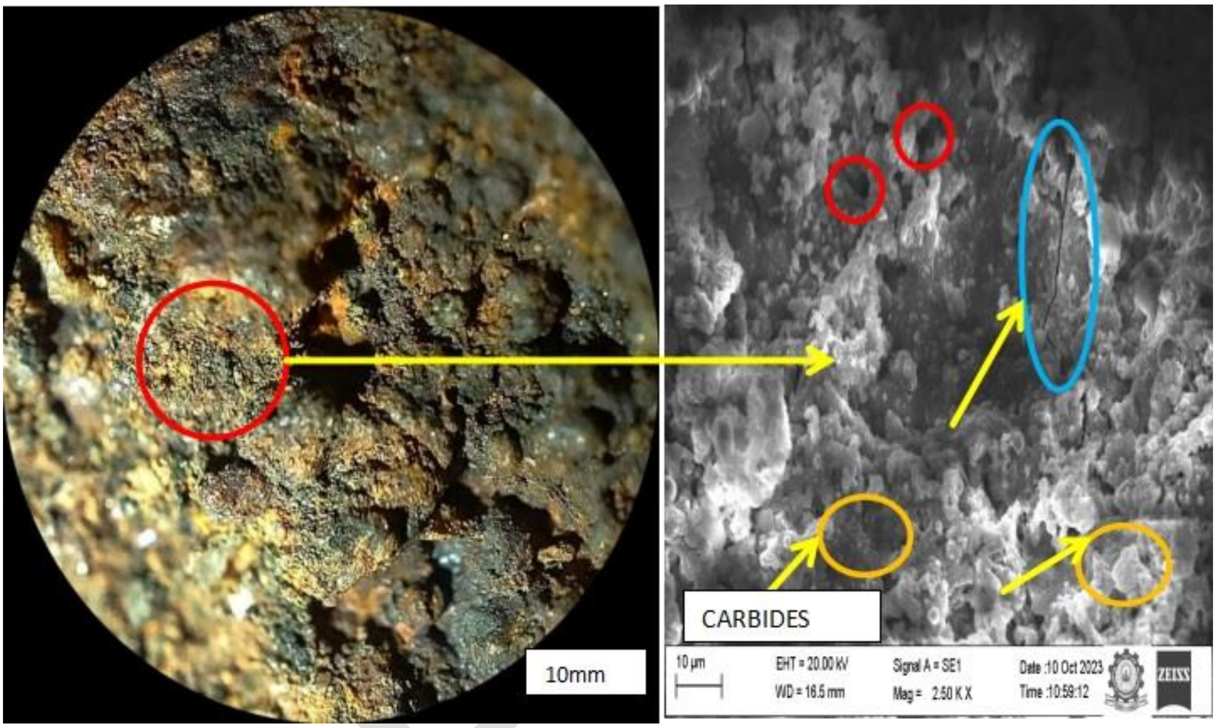

Fig. 4: (a) Macroscopic fracture morphology and (b) SEM fracture morphology of GS-42CrMo4V steel, with appropriate scale bars.

The fracture surface exhibited numerous dimple-like features and microvoids. These features indicate that microvoid nucleation, growth and coalescence contributed substantially to the fracture process. Localized particle-associated pull-out regions and secondary cracking were also observed.

The predominance of dimpled morphology indicates a substantial ductile component in the fracture process. The localized cracking and particle-associated regions suggest that microstructural heterogeneity may have influenced crack initiation and propagation. The fractographic observations are therefore consistent with the tensile results, which showed substantial tensile strength together with measurable deformation before fracture.

2.6 Electrochemical Corrosion Behaviour

Electrochemical characterization was performed to evaluate the corrosion response of the GS-42CrMo4V steel under chloride-containing and acidic environments [13]. Before testing, the specimens were ground progressively to 2400 grit, cleaned with acetone, rinsed with distilled water and dried under ambient conditions.

Electrochemical measurements were conducted using a VersaSTAT 4 electrochemical workstation with a conventional three-electrode cell. The exposed specimen area was 2 cm × 2 cm. A silver/silver-chloride reference electrode and platinum counter electrode were used with the GS-42CrMo4V specimen as the working electrode. The electrochemical tests were performed after stabilization of the open-circuit potential for approximately 30 min.

The investigated electrolytes were 3.5 wt.% NaCl, 0.1 M HCl, 0.5 M HCl, 0.1 M H_2SO_4 and 0.5 M H_2SO_4. These environments provide a comparison between chloride-containing and acidic conditions.

2.6.1 Potentiodynamic Polarization Behaviour

Potentiodynamic polarization measurements were performed using a scan rate of 1 mV s^{-1} after open-circuit stabilization. The corrosion potential, corrosion current density, cathodic and anodic Tafel slopes, and corrosion rate were obtained from the polarization curves. The polarization curves for the investigated electrolytes are presented in Fig. 5, and the corresponding electrochemical parameters are listed in Table 4.

Table 4. Potentiodynamic polarization parameters of GS-42CrMo4V steel

Electrolyte	Ecorr (mV)	Icorr (μA cm^{-2})	βc (mV dec^{-1})	βa (mV dec^{-1})	Corrosion rate (mpy)	Potential range (mV)
3.5 wt.% NaCl	−639.033	1.597	99.883	99.883	0.487	−913.0 to −413.1
0.1 M HCl	−510.399	162.759	90.906	90.906	51.317	−764.6 to −265.6
0.5 M HCl	−477.539	313.382	94.632	94.632	95.502	−725.6 to −228.8

[DOI: 10.22068/ijmse.4652]

Electrolyte	Ecorr (mV)	Icorr (μA cm⁻²)	βc (mV dec⁻¹)	βa (mV dec⁻¹)	Corrosion rate (mpy)	Potential range (mV)
0.1 M H_2SO_4	−495.933	352.026	99.351	98.635	107.280	−738.8 to −240.4
0.5 M H_2SO_4	−471.570	311.262	92.126	61.349	94.856	−717.0 to −224.5

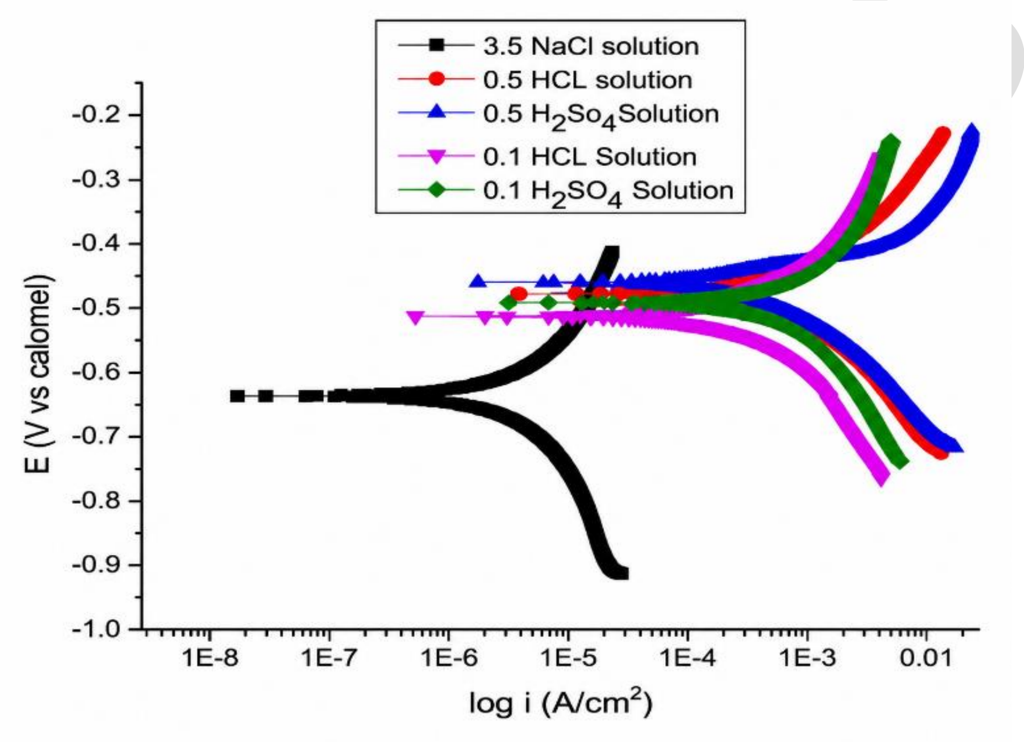

Fig. 5. Potentiodynamic polarization curves of GS-42CrMo4V steel in the investigated electrolytes.

The polarization response was strongly dependent on the electrolyte. The lowest corrosion current density was obtained in 3.5 wt.% NaCl, with an Icorr of 1.597 μA cm⁻² and a calculated corrosion rate of 0.487 mpy. The acidic electrolytes produced substantially higher corrosion current densities, ranging from 162.759 to 352.026 μA cm⁻².

The highest corrosion current density was measured in 0.1 M H_2SO_4. The 0.5 M H_2SO_4 solution produced a slightly lower corrosion current density of 311.262 μA cm⁻². Thus, the corrosion response

[DOI: 10.22068/ijmse.4652]

was influenced not only by acid concentration but also by the nature of the electrolyte and the reactions occurring at the steel-electrolyte interface.

The substantially higher corrosion activity in acidic environments can be associated with accelerated anodic dissolution and cathodic hydrogen-evolution reactions. The polarization results consequently demonstrate that the investigated GS-42CrMo4V steel has considerably greater electrochemical stability in the investigated chloride environment than in the acidic electrolytes.

2.6.2 Electrochemical Impedance Spectroscopy

Electrochemical impedance spectroscopy was conducted to further characterize the steel-electrolyte interface. The measurements were performed over a frequency range from 100 kHz to 0.01 Hz using a sinusoidal perturbation amplitude of 10 mV. The Nyquist and Bode responses are presented in Fig. 6 and Fig. 7, respectively.

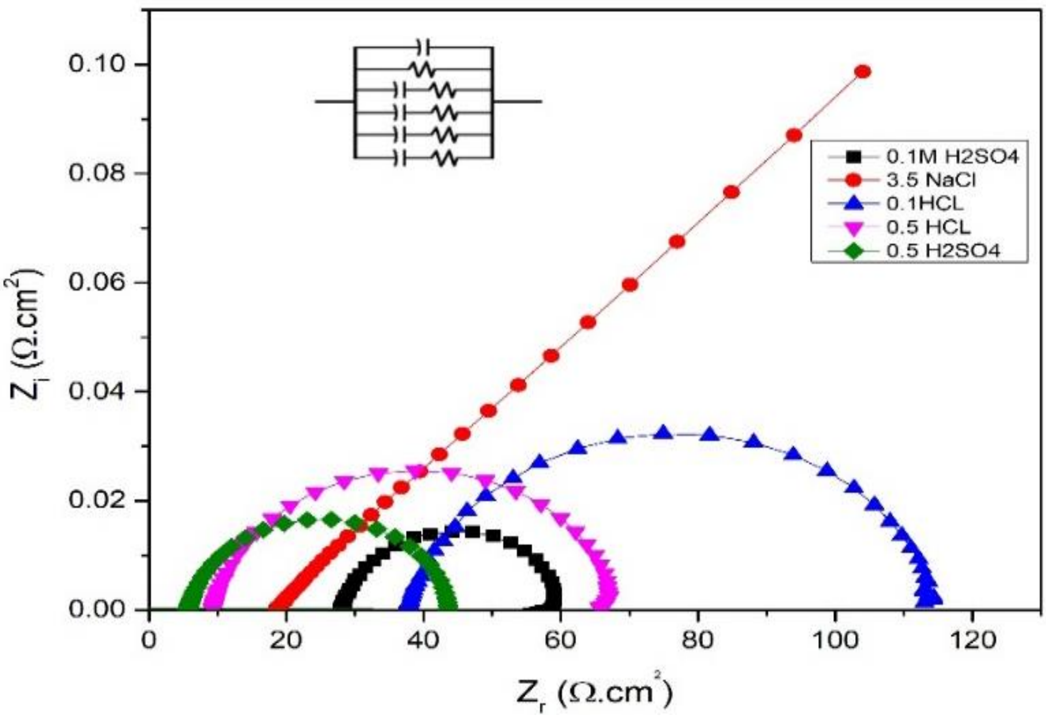

Fig. 6. Nyquist plots obtained from EIS measurements of GS-42CrMo4V steel in the investigated electrolytes.

[DOI: 10.22068/ijmse.4652]

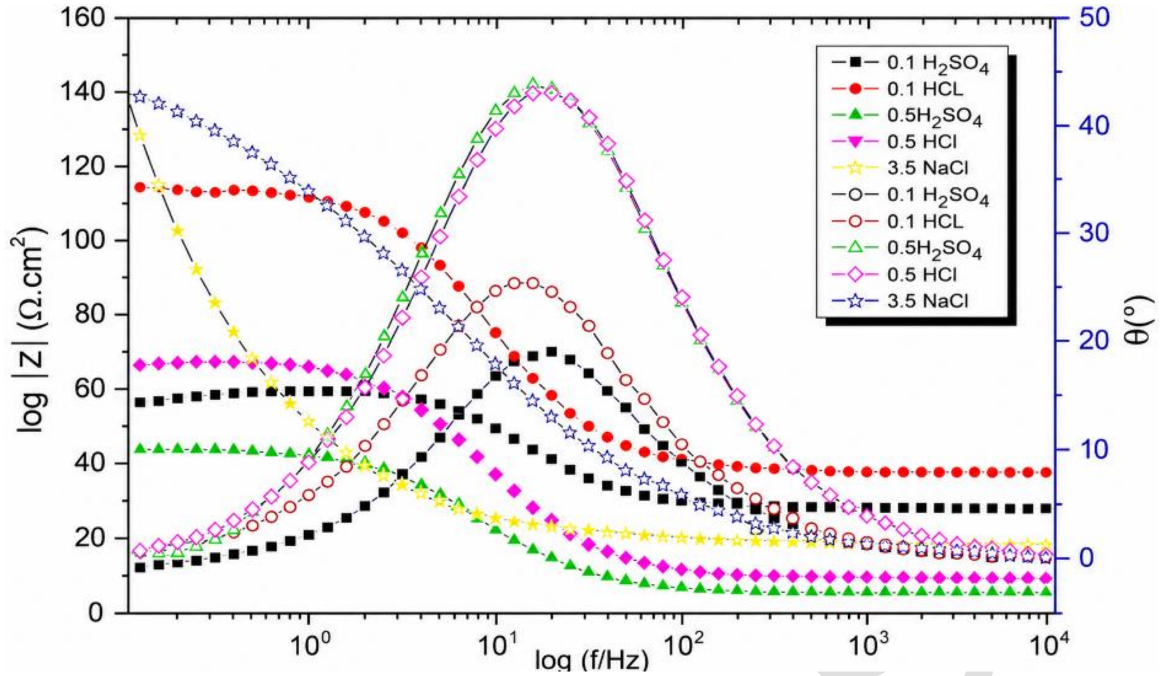

Fig. 7. Bode plots obtained from EIS measurements of GS-42CrMo4V steel in the investigated electrolytes.

The Nyquist plots exhibited predominantly capacitive arcs, with the largest response observed for the 3.5 wt.% NaCl environment. A larger capacitive arc corresponds to a greater impedance of the electrochemical interface and therefore indicates greater resistance to charge transfer under the corresponding test condition [16].

The impedance response was analysed using an equivalent electrical circuit consisting of solution resistance (Rs) in series with a parallel combination of charge transfer resistance (Rct) and a constant phase element (CPE) [14], [17]. The CPE was used instead of an ideal capacitor to account for non-ideal capacitive behaviour at the metal electrolyte interface [14]. Where the low-frequency response exhibited diffusion characteristics, a Warburg impedance element was considered.

The fitting procedure produced a reported chi-square value of 6.933×10^{-5}, with the reported fitting error below 10%. The larger impedance response observed for the NaCl environment is consistent with the substantially lower corrosion current density obtained from the polarization measurements.

The EIS results therefore provide independent qualitative support for the polarization results: the steel-electrolyte interface exhibited comparatively greater resistance to electrochemical charge transfer in 3.5

wt.% NaCl, whereas the acidic environments produced lower interfacial impedance and substantially greater corrosion activity.

2.7 Three-Body Abrasion Behaviour

Three-body abrasion testing was performed to evaluate the resistance of GS-42CrMo4V steel to material removal caused by loose abrasive particles. The test was based on the dry-sand/rubber-wheel principle described in ASTM G65 [18]. The specimen dimensions were 75.6 × 25.4 × 12.7 mm and the material density was 7.82 g cm^{-3}. AFS 50-grade sand was supplied at a flow rate of 350 g min^{-1}. The rubber wheel was operated at 200 rpm for 6000 revolutions, corresponding to a test duration of approximately 30 min. An applied mass of 4.1 kg was used during the test, corresponding to an equivalent gravitational force of approximately 40.2 N. The test parameters are summarized in Table 5.

Table 5. Three-body abrasion test parameters

Parameter	Value
Test material	GS-42CrMo4V steel
Specimen size	75.6 × 25.4 × 12.7 mm
Density	7.82 g cm^{-3}
Applied mass	4.1 kg
Equivalent gravitational force	≈40.2 N
Wheel speed	200 rpm
Number of revolutions	6000
Abrasive	AFS 50 sand
Sand flow rate	350 g min^{-1}
Test duration	30 min

[DOI: 10.22068/ijmse.4652]

The initial and final masses and the calculated material loss are presented in Table 6.

Table 6. Three-body abrasion result of GS-42CrMo4V bottom roller material

Trial	Initial mass (g)	Final mass (g)	Mass loss (g)	Volume loss (mm^3)
1	186.803	185.295	1.508	192.83

The specimen exhibited a mass loss of 1.508 g, corresponding to a volume loss of 192.83 mm^3. The result confirms measurable abrasive material removal under the selected test conditions despite the relatively high hardness of the roller material.

Material removal under three-body abrasion can occur through abrasive particle penetration, micro-cutting, ploughing and repeated near-surface deformation [8], [9]. The observed result demonstrates that the abrasive response of the steel is governed by the combined effects of hardness, microstructure, abrasive characteristics and contact conditions rather than hardness alone [10], [11].

2.8 Linear Reciprocating Wear Behaviour

Linear reciprocating wear testing was performed to evaluate the sliding wear response of the bottom roller material under different normal loads and temperatures [12], [19]. The test was conducted with a stroke length of 7 mm, a frequency of 15 Hz and a duration of 900 s. Normal loads of 25, 50 and 75 N were applied at temperatures of 30, 60 and 90 °C. The test conditions are summarized in Table 7.

Table 7. Linear reciprocating wear test parameters

Parameter	Value
Stroke length	7 mm
Frequency	15 Hz
Test duration	900 s
Total sliding distance	189 m

[DOI: 10.22068/ijmse.4652]

Parameter	Value
Normal loads	25, 50 and 75 N
Test temperatures	30, 60 and 90 °C
Number of specimens	Three per condition

The total sliding distance was calculated as:

$$L = 2Sft$$

where S is the stroke length, f is the reciprocating frequency and t is the test duration. For the present test conditions,

$$L = 2(7)(15)(900) = 189000 \text{ mm} = 189 \text{ m}.$$

The specific wear rate was determined from:

$$K = \frac{V}{FL}$$

where K is the specific wear rate, V is the wear volume, F is the applied normal load and L is the sliding distance. The measured wear results are presented in Table 8.

Table 8. Linear reciprocating wear results of GS-42CrMo4V bottom roller

Load (N)	Temperature (°C)	Mass loss (g)	Volume loss (mm^3)	Specific wear rate ($mm^3 N^{-1} m^{-1}$)
25	30	0.0010	0.127877	2.71×10^{-5}
50	30	0.0015	0.191816	2.03×10^{-5}
75	30	0.0016	0.204604	1.44×10^{-5}
25	60	0.0012	0.153453	3.25×10^{-5}

[DOI: 10.22068/ijmse.4652]

Load (N)	Temperature (°C)	Mass loss (g)	Volume loss (mm^3)	Specific wear rate ($mm^3\ N^{-1}\ m^{-1}$)
50	60	0.0012	0.153453	1.62×10^{-5}
75	60	0.0017	0.217391	1.53×10^{-5}
25	90	0.0030	0.383632	8.11×10^{-5}
50	90	0.0040	0.511509	5.41×10^{-5}
75	90	0.0041	0.524297	3.70×10^{-5}

At 30 °C, the mass loss increased from 0.0010 g at 25 N to 0.0016 g at 75 N. At 60 °C, the mass loss ranged from 0.0012 to 0.0017 g. A substantially greater material loss was observed at 90 °C, where the mass loss increased from 0.0030 g at 25 N to 0.0041 g at 75 N.

The effect of temperature is also evident in the calculated specific wear rate. At 25 N, the wear rate increased from 2.71×10^{-5} $mm^3\ N^{-1}\ m^{-1}$ at 30 °C to 8.11×10^{-5} $mm^3\ N^{-1}\ m^{-1}$ at 90 °C. At 50 N, it increased from 2.03×10^{-5} to 5.41×10^{-5} $mm^3\ N^{-1}\ m^{-1}$, while at 75 N it increased from 1.44×10^{-5} to 3.70×10^{-5} $mm^3\ N^{-1}\ m^{-1}$.

The results therefore demonstrate a strong temperature dependence of the sliding-wear response. The increase in wear at 90 °C may be associated with temperature-induced changes in near-surface mechanical behaviour, oxide formation, frictional conditions and the stability of the contacting surfaces [12], [20].

Although the absolute mass and volume losses generally increased with increasing load, the calculated specific wear rate decreased with load at each investigated temperature [12]. This distinction is important because specific wear rate is normalized by both load and sliding distance. Consequently, the increase in absolute material removal with load does not necessarily correspond to an increase in the normalized wear coefficient.

The combined wear results show that GS-42CrMo4V maintains relatively low material loss under the lower-temperature conditions investigated, whereas elevated temperature produces a marked increase in wear. The results demonstrate the importance of considering both mechanical loading and temperature when assessing the tribological suitability of the material for crawler undercarriage applications.

3. Discussions

The individual experiments presented in Section 2 describe different aspects of the behaviour of the service-exposed GS-42CrMo4V bottom roller. Their significance becomes clearer when the mechanical, electrochemical and tribological responses are considered together. In service, these properties do not act independently. The roller must retain sufficient surface hardness to resist abrasive penetration, adequate strength and deformation capacity to sustain repeated loading, and reasonable resistance to environmental attack. The present results therefore point to a balance of properties rather than a single controlling material parameter.

3.1 Composition, Hardness and Mechanical Response

The measured composition of the investigated steel, particularly its carbon, chromium and molybdenum contents, is consistent with a low-alloy cast steel capable of developing high hardness and strength following suitable heat treatment. The service-exposed bottom roller retained an average microhardness of 430.0 ± 10.6 HV, appreciably higher than the 314.2 ± 5.6 HV measured for the roller pin. This difference agrees with the functional requirement of the roller working surface, which is subjected directly to rolling contact and abrasive interaction.

The tensile results, however, show that higher hardness does not necessarily correspond to higher tensile strength. The bottom roller exhibited a mean UTS of 773.3 ± 10.7 MPa, whereas the roller pin reached 944.0 ± 48.9 MPa. The two measurements characterize different responses: hardness reflects resistance to localized indentation and plastic deformation, while tensile strength describes resistance to failure under uniaxial loading. Their different trends therefore emphasize the need to evaluate the components according to their individual service functions rather than rank them using one mechanical property.

[DOI: 10.22068/ijmse.4652]

For the bottom roller, a hard working region is advantageous because penetration and ploughing by mineral particles are important sources of surface damage. The underlying material must nevertheless retain sufficient mechanical integrity to accommodate the stresses transferred from the hardened surface. Increasing hardness indiscriminately would therefore not necessarily improve service performance [11]. A more useful objective is to maintain a stable hardened surface supported by material capable of sustaining repeated loading without premature cracking.

The fractographic observations reinforce this interpretation. Dimpled regions and microvoid features indicate that localized plastic deformation and microvoid coalescence contributed to tensile fracture. At the same time, particle-associated features and secondary cracks reveal local heterogeneity in the fracture process. Such sites can become important under repeated loading because local discontinuities may act as stress concentrators. The mechanical response of the roller is consequently governed not only by its nominal hardness or strength but also by the uniformity of the cast and heat-treated microstructure.

3.2 Environmental Dependence of Corrosion Behaviour

A marked difference was observed between the corrosion behaviour in 3.5 wt.% NaCl and that in the acidic electrolytes. The corrosion current density in NaCl was only 1.597 μA cm^{-2}, compared with values between 162.759 and 352.026 μA cm^{-2} in the HCl and H_2SO_4 solutions. The corresponding calculated corrosion rate increased from 0.487 mpy in NaCl to 51.317–107.280 mpy in the acidic environments. The electrochemical stability of the investigated steel is therefore strongly dependent on the surrounding medium.

The acid-concentration response was not entirely monotonic. For example, 0.1 M H_2SO_4 produced a higher corrosion current density than 0.5 M H_2SO_4. It would consequently be inappropriate to explain the results simply in terms of increasing acid concentration. Electrolyte chemistry, interfacial reactions and the condition of corrosion products formed on the surface can all influence the measured electrochemical response.

The impedance measurements support the polarization behaviour. The comparatively larger impedance response in the NaCl environment indicates greater resistance to interfacial charge transfer, whereas the

[DOI: 10.22068/ijmse.4652]

acidic solutions exhibited lower impedance and considerably greater corrosion activity. Agreement between the polarization and EIS observations strengthens the conclusion that the steel is much more vulnerable under the acidic conditions investigated.

These findings have practical implications for mining components. A mechanically adequate roller can still undergo accelerated deterioration if its surface is exposed to an aggressive environment. Water, dissolved salts and chemically aggressive contaminants may reach worn or damaged regions during service. Once the working surface has been mechanically disturbed, fresh material becomes exposed and the contribution of corrosion to subsequent degradation can increase. Corrosion resistance must therefore be considered together with mechanical and tribological properties when evaluating the durability of the roller.

3.3 Abrasive and Sliding Wear Response

The three-body abrasion test produced a volume loss of 192.83 mm^3 despite the relatively high hardness of the roller material. This result demonstrates an important limitation of using hardness alone as an indicator of wear resistance [11], [21]. A hard surface can restrict abrasive penetration, but loose mineral particles can still cause material removal through repeated indentation, ploughing and cutting. The response will also depend on particle characteristics, microstructural condition and the manner in which the abrasive interacts with the surface[8], [10].

The reciprocating tests provide a clearer indication of the influence of operating conditions. Absolute material loss generally increased with applied load, but the effect of temperature was considerably more pronounced. At 25 N, for example, the measured volume loss increased from 0.127877 mm^3 at 30 °C to 0.383632 mm^3 at 90 °C. At 75 N, it increased from 0.204604 to 0.524297 mm^3 over the same temperature interval. The deterioration at 90 °C shows that the wear response of the steel cannot be assessed adequately from room-temperature behaviour alone [12], [20].

The specific wear rate followed a different trend from absolute material loss. At each investigated temperature, the normalized wear rate generally decreased as normal load increased. At 30 °C, it decreased from 2.71×10^{-8} $mm^3\ N^{-1}\ m^{-1}$ at 25 N to 1.44×10^{-8} $mm^3\ N^{-1}\ m^{-1}$ at 75 N. A similar pattern

[DOI: 10.22068/ijmse.4652]

was observed at 60 and 90 °C. Since specific wear rate is normalized with respect to both applied load and sliding distance, an increase in absolute material loss does not necessarily result in an increase in the normalized value. The two quantities should therefore be considered together.

The strong temperature dependence is particularly relevant to the roller application. Repeated contact and sliding can generate localized frictional heating, while the evolving surface may undergo deformation, oxidation and repeated removal of wear debris. The present results establish the increase in material loss with temperature; however, attribution of this increase to a particular microscopic wear mechanism would require corresponding wear-track microstructural or compositional evidence.

3.4 Interaction of Mechanical Wear and Corrosion

The mechanical and electrochemical results together indicate that service degradation should not be treated as separate wear and corrosion problems. Abrasion and repeated sliding alter the surface condition of the roller, while environmental exposure can attack the newly exposed material. Surface degradation caused by one process may therefore increase susceptibility to another [15].

Abrasive particles can initially produce grooves, local deformation and removal of material from the working surface. Repeated contact can extend this damage and continuously expose fresh steel. In the presence of moisture or aggressive species, these exposed areas provide locations for electrochemical dissolution. Corrosion can subsequently increase surface irregularity and introduce local discontinuities, which may become preferential sites for further mechanical damage.

This interpretation is especially relevant in view of the substantially greater corrosion activity measured in acidic solutions. Under a relatively mild environment, mechanical wear may remain the more prominent degradation process. If the same mechanically damaged surface is exposed to an acidic medium, electrochemical degradation can become much more significant.

The present experiments evaluated corrosion and wear separately; therefore, a quantitative synergistic wear-corrosion rate cannot be derived from the current data. Nevertheless, the individual responses demonstrate that both mechanisms are relevant to the material and that environmental severity can substantially change the condition of a mechanically loaded surface. This distinction is important because it avoids attributing a quantitatively measured tribocorrosion mechanism to experiments that were not performed simultaneously.

3.5 Implications for Bottom-Roller Performance

Taken together, the results show why selection of a track-roller material cannot be based solely on hardness, tensile strength, corrosion resistance or laboratory wear rate [4]. The service-exposed bottom roller retained a relatively hard working condition and substantial tensile strength, while the fracture morphology showed a considerable ductile component. These characteristics are favourable for a component required to resist surface deformation without behaving as a completely brittle material.

There are, however, identifiable limitations. The material remains susceptible to three-body abrasion, sliding material loss increases considerably at elevated temperature, and corrosion resistance deteriorates sharply in acidic media. The combination of these responses is more important for service performance than the maximum value of any individual property.

The contrast between the bottom roller and roller pin illustrates this point. The pin exhibited greater tensile strength but considerably lower hardness. It cannot therefore be concluded that the pin possesses superior overall material performance. Each component has a different function and consequently requires a different property balance. For the roller, resistance to surface degradation is particularly important, while sufficient supporting strength and resistance to fracture must be retained beneath the working region.

A suitable material condition for this application can therefore be described as a hard and wear-resistant working surface supported by a mechanically reliable interior, together with sufficient environmental resistance for the anticipated service conditions.

3.6 Material and Process Improvement Strategy

The results provide several routes for improving the performance of the bottom roller. These improvements should be directed toward balancing the relevant properties rather than simply increasing hardness or strength.

[DOI: 10.22068/ijmse.4652]

The first consideration is control of the hardened working region. The measured hardness confirms that the service-exposed roller retained a comparatively hard surface condition. Further improvement should therefore focus on achieving a uniform and stable hardened layer rather than pursuing the highest attainable hardness. Control of the quenching, tempering and surface-hardening operations is important because local variations in hardness or microstructure can result in uneven wear and local stress concentration [6], [13].

Casting quality is equally important. The particle-associated features and localized secondary cracking observed during fractographic examination indicate that local heterogeneity can participate in the fracture process. Improved melt cleanliness, control of inclusions and minimization of casting discontinuities would reduce potential sites for microvoid formation and crack initiation. Uniformity of the subsequent heat-treatment response is also required so that the mechanical behaviour does not vary substantially across critical regions of the component.

The corrosion results identify environmental resistance as another area requiring attention. Because the corrosion activity increased sharply in the acidic solutions, protection of the working material from aggressive chemical exposure can contribute to longer component life. Where such exposure occurs, control of retained moisture and corrosive deposits should accompany material improvements. Surface-protection systems may also be considered, provided that they can withstand the contact and abrasive conditions without compromising the required dimensions or mechanical integrity of the roller surface [22].

The reciprocating results further indicate that thermal conditions should form part of the improvement strategy. Material loss increased markedly at 90 °C. Measures that reduce frictional heating, maintain effective lubrication and improve dissipation of heat from the contact region may therefore help preserve the working surface during prolonged operation [12].

The experimental findings ultimately favour an optimization strategy based on surface hardness, supporting strength and toughness, microstructural uniformity, wear resistance and environmental stability considered together. For GS-42CrMo4V bottom rollers, controlled heat treatment and

[DOI: 10.22068/ijmse.4652]

hardened-layer characteristics, improved casting cleanliness, mitigation of aggressive environmental exposure and control of frictional heating provide more technically balanced routes for improvement than maximizing any one material property. This integrated approach directly reflects the multiple degradation processes encountered by a track roller and provides a more appropriate basis for improving its service durability.

4. Conclusions

The present study evaluated the mechanical, electrochemical and tribological behaviour of service-exposed GS-42CrMo4V cast steel used for a bucket-wheel excavator bottom roller. The material exhibited a relatively high average microhardness of 430.0 ± 10.6 HV, while the roller pin showed a lower hardness of 314.2 ± 5.6 HV but a higher average ultimate tensile strength of 944.0 ± 48.9 MPa compared with 773.3 ± 10.7 MPa for the bottom roller, confirming that hardness and tensile strength provide different measures of material performance. Fractographic examination revealed predominantly ductile fracture characteristics with dimple-like features and localized microvoid-related deformation, together with localized particle-associated damage and secondary cracking. The electrochemical results demonstrated substantially better corrosion resistance in 3.5 wt.% NaCl, where the corrosion current density was 1.597 μA/cm² and the calculated corrosion rate was 0.487 mpy, whereas considerably higher corrosion activity was observed in the investigated HCl and H_2SO_4 environments. The three-body abrasion test confirmed measurable material removal, while the reciprocating wear tests showed that temperature had a pronounced influence on material loss, with substantially greater wear at 90 °C than at 30 °C. Overall, the findings demonstrate that the service performance of GS-42CrMo4V bottom rollers is governed by the combined effects of surface hardness, mechanical strength, fracture behaviour, abrasive wear, sliding wear and environmental exposure rather than by any single material property. The results therefore support a balanced improvement strategy involving controlled heat treatment and hardened-layer characteristics, improved casting and microstructural uniformity, protection against aggressive environments, and control of frictional heating during service. Such an integrated approach can enhance the reliability and durability of GS-42CrMo4V rollers subjected to the simultaneous

[DOI: 10.22068/ijmse.4652]

mechanical, tribological and environmental conditions encountered in bucket-wheel excavator applications.

5. References

1. Singh, A., Sendil Kumar, C. and Das, P., "Finite element modelling of deformation behaviour and failure analysis of roller and pin assembly in bucket wheel excavators used in opencast coal mines," *Eng. Fail. Anal.*, 2024, 164, 108677.
2. Yan, B. J., Zhang, Z. H., Zhang, H. Q., Zhang, W. J., Zhao, Z. D. and Yang, T., "Dynamic Contact Characteristics Analysis of Heavy-duty Track Rollers," *Int. J. Automot. Mech. Eng.*, 2024, 21, 11155–11165.
3. Zhou, L., Qu, Q., Wang, C. and Zhang, H., "Finite element analysis of track rollers of the crawler excavator based on ANSYS," *Key Eng. Mater.*, 2011, 467–469, 1803–1807.
4. Autay, R., Kchaou, M., Elleuch, K. and Dammak, F., "Tribological behaviour of carbon and low alloy steels: Effect of mechanical properties and test conditions," *Tribol. Mater. Surf. Interfaces*, 2011, 5, 133–140.
5. Haiko, O., Javaheri, V., Valtonen, K., Kaijalainen, A., Hannula, J. and Kömi, J., "Effect of prior austenite grain size on the abrasive wear resistance of ultra-high strength martensitic steels," *Wear*, 2020, 454–455, 203336.
6. Cao, Y. J., Sun, J. Q., Ma, F., Chen, Y. Y., Cheng, X. Z., Gao, X. and Xie, K., "Effect of the microstructure and residual stress on tribological behavior of induction hardened GCr15 steel," *Tribol. Int.*, 2017, 115, 108–115.
7. Holmberg, K., Kivikytö-Reponen, P., Härkisaari, P., Valtonen, K. and Erdemir, A., "Global energy consumption due to friction and wear in the mining industry," *Tribol. Int.*, 2017, 115, 116–139.
8. Li, Y., Schreiber, P., Schneider, J. and Greiner, C., "Tribological mechanisms of slurry abrasive wear," *Friction*, 2023, 11, 1079–1093.
9. Meng, Y., Xu, J., Jin, Z., Prakash, B. and Hu, Y., "A review of recent advances in tribology," *Friction*, 2020, 8, 221–300.

[DOI: 10.22068/ijmse.4652]

10. Stachowiak, G. and Stachowiak, G., "The effects of particle characteristics on three-body abrasive wear," *Wear*, 2001, 249, 201–207.

11. Zdravecká, E., Tkáčová, J. and Ondáč, M., "Effect of microstructure factors on abrasion resistance of high-strength steels," *Res. Agr. Eng.*, 2014, 60, 115–120.

12. Autay, R., Kchaou, M. and Dammak, F., "Experimental investigation of the tribological behaviour of carbon and low-alloy steels sliding against HSS," *Mech. Ind.*, 2015, 16, 109.

13. Hanza, S. S., Štic, L., Liverić, L. and Špada, V., "Corrosion Behaviour of Tempered 42CrMo4 Steel," *Mater. Tehnol.*, 2021, 55, 427–433.

14. Solomon, M. M., Onyeachu, I. B., Njoku, D. I., Nwanonenyi, S. C. and Oguzie, E. E., "Adsorption and corrosion inhibition characteristics of 2–(chloromethyl)benzimidazole for C1018 carbon steel in a typical sweet corrosion environment: Effect of chloride ion concentration and temperature," *Colloids Surf. A Physicochem. Eng. Asp.*, 2021, 610, 125638.

15. Jiang, J., Islam, M. A., Xie, Y. and Stack, M. M., "Some Thoughts on Modeling Abrasion-Corrosion: Wear by Hard Particles in Corrosive Environments," *J. Bio Tribo Corros.*, 2024, 10, 12.

16. Xu, P., Zhao, M., Fu, X. and Zhao, C., "Effect of chloride ions on the corrosion behavior of carbon steel in an iron bacteria system," *RSC Adv.*, 2022, 12, 15158–15166.

17. Chauhan, D. S., Quraishi, M. A., Sorour, A. A., Saha, S. K. and Banerjee, P., "Triazole-modified chitosan: A biomacromolecule as a new environmentally benign corrosion inhibitor for carbon steel in a hydrochloric acid solution," *RSC Adv.*, 2019, 9, 14990–15003.

18. Das Bakshi, S., Shipway, P. H. and Bhadeshia, H. K. D. H., "Three-body abrasive wear of fine pearlite, nanostructured bainite and martensite," *Wear*, 2013, 308, 46–53.

19. Zhang, H., Que, B., Dong, L., Li, Z., Cheng, Y. and Wang, X., "Unraveling the Friction and Wear Mechanisms of a Medium-Carbon Steel with a Gradient-Structured Surface Layer," *Lubricants*, 2025, 13, 448.

20. Chowdhury, M. A., Nuruzzaman, D. M. and Chowdhury, M. A., "Experimental Investigation on Friction and Wear Properties of Different Steel Materials," *Tribol. Ind.*, 2013, 35, 42–50.

[DOI: 10.22068/ijmse.4652]

21. Sun, H., Zhou, Y., Liao, X. and Li, A., “Abrasive wear characteristics of 40Mn2 steel in simulated condition of sprocket wheel in crawler bulldozer walking system,” *Surf. Topogr.*, 2019, 7, 031004.

22. Doan, T. V., Kusmič, D., Pospíchal, M., Tran, Q. D. and Nguyen, V. T., “Friction and Wear Behaviour of 42CrMo4 Steel Treated by Tenifer, Hard Chrome and Plasma Nitriding Technologies,” *Manuf. Technol.*, 2017, 17, 168–174.

[DOI: 10.22068/ijmse.4652]